J. Membrane Biol. 121 – 134 (1978)

Power Density Spectra of Frog Skin Potential, Current and Admittance Functions during Patch Clamp

T. Hoshiko

Department of Physiology, Case Western Reserve University, School of Medicine, Cleveland, Ohio 44106

Received 30 November 1977

Summary. Clamp current fluctuations in frog skin of areas down to 0.07 cm^2 are dominated by low frequency components (< 100 Hz). Patch clamp of 0.001 cm^2 under high density fluorosilicone oil exhibits components up to 5000 Hz, often including a peak in the current power density spectrum. The admittance spectrum also exhibits a peak at the same frequency. In some skins no peak was observed, but the break in the curve was too sharp to be Lorentzian. In all instances the final limiting slope approached $1/f^2$. The resonance peak was observed in either Cl^- or $SO_4^=$ Ringer's but disappeared when Na^+ was replaced with K^+. Resonance frequency varied from 100 to 700 Hz.

Professor Ussing first described his now classical model of frog skin with V. Koefoed-Johnson at the XX International Physiological Congress in Brussels in 1956 (Ussing & Koefoed-Johnson, 1956; Koefoed-Johnson & Ussing, 1958).

One feature of that model, the sodium selective nature of the apical border of frog skin and toad bladder, has been studied recently by following the fluctuations in open circuit potential (Segal, 1972; Van Driessche & Borghgraef, 1975) and short-circuit current (Hoshiko, 1975; Strandberg & Hammer, 1975; Lindemann, 1976; Lindemann & Van Driessche, 1977). In all these previous studies, relatively large areas have been observed, and only low frequency components (< 100 Hz) have been reported. In nerve, noise power components up to 5000 Hz have been reported in the isolated node of Ranvier (Derksen, 1965; Derksen & Verveen, 1966), with sucrose gap in lobster axon (Poussart, 1969; 1971), with air-gap "node" (Wanke, DeFelice & Conti, 1974; Conti, DeFelice & Wanke, 1975), and with patch clamp (Fishman, Moore & Poussart, 1975*a*; Fishman, Poussart & Moore, 1975*b*; Fishman, 1975) in squid axon. In this report, I describe fluctuations up to 5000 Hz as well as resonance behavior at the apical membrane of isolated frog skin made

0022-2631/78/S040-0121 $02.80

possible by use of a patch clamp with a nonaqueous, nonconductive medium for electrical isolation.

Materials and Methods

Abdominal skins of *Rana pipiens* (northern variety), obtained from Mogul Ed, Oshkosh, Wisconsin and from Bay Biologicals, Port Credit, Ontario, were used. In "large area" preparations abdominal skin was sandwiched between polyethylene sheets (0.76 mm thick) coated with Dow Corning high vacuum silicone grease. A central area in the polyethylene sheet (1 cm in diameter) was thinned to ca. 0.3 mm, and a 3-mm diameter circular hole was cut in each sheet. The holes were aligned opposite each other. The skin-polyethylene sandwich was clamped lightly between "U-shaped" troughs cut in Lucite. The preparations probed with the patch clamp pipette were mounted on a micropuncture chamber similar to that used by Seldin and Hoshiko (1966), except that a Lucite ring was used to hold down the skin, and current and potential bridges were inserted in the lower chamber. The exposed area was about 0.6 cm^2.

Calomel cells were used to measure the potential across the skin and silver-silver chloride electrodes were used to pass current.

For the patch clamp (Fig. 1), double pipettes were pulled by hand from 1-mm diameter borosilicate glass to give tip diameters of about 0.1 mm. The area under the

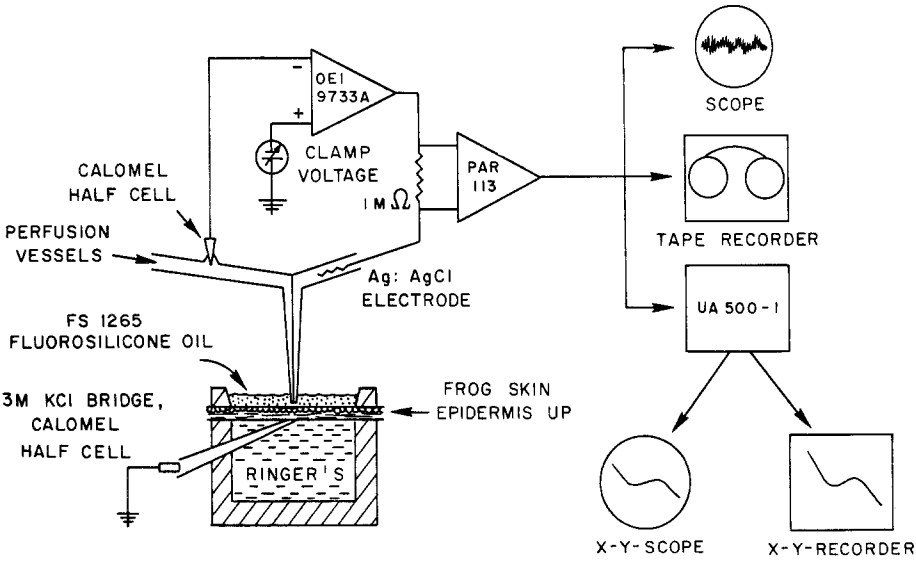

Fig. 1. Patch clamp system for frog skin. Patch clamp accomplished with a double pipette. The clamp amplifier (OEI 9733A) and PAR 113 were battery powered separately and placed along with the chamber in a small steel case. The case itself was placed on a weighted platform floated on air-inflated automobile inner tubes. The natural frequency of the platform was under 1 Hz. In most cases, a second clamp amplifier was used to hold the solution bathing the lower, basolateral or corium surface at ground potential (*cf.* Menninger, Snell & Spangler, 1960). *See text* for further details [Reprinted with permission of Raven Press from Hoshiko + Moore, 1978. (Membrane Transport Kinetics, Vol. 1, p. 179. J.F. Hoffman, editor)]

clamp was estimated from the observed time constant and DC patch resistance by calculating the capacitance and assuming a specific capacitance of $2\,\mu F/cm^2$ (Smith, 1975). The current pipette was filled with 1% agar in 1 N K_2SO_4. The upper end was filled with 3 M KCl and a chlorided silver wire was sealed in. The potential pipette was mounted on a micromanipulator and attached to a perfusion system. A calomel electrode with a fiber tip or sintered glass junction made contact with the perfusion stream through a T-connection. The DC resistance of the potential measuring pipette system was about 1 MΩ, and that of the current pipette was about 100 kΩ. The resistances of the electrodes and bridges connected to the lower chamber were about 5 kΩ. The electrode bridge resistances in the "large area" preparation were all about 5 kΩ also.

The skin apical surface in the micropuncture chamber was blotted dry and covered with a fluorosilicone fluid (Dow Corning FS1265) of 1.25 density. The double pipette was lowered through the surface of the fluorosilicone and put in contact with the skin surface at an angle of ca. 80°. The surface and pipette were observed through a dissection microscope at magnifications of 10–40×.

Solutions used were half strength sodium sulfate Ringer's (in meq/liter: Na, 55; K, 5; Ca, 1; Tris, 5; pH 7.8), half strength Tris-sulfate Ringer's (same composition but Na replaced by Tris), NaCl-Ringer's (in meq/liter: Na, 115; K, 5; Ca, 1; Tris, 5; pH 7.7) and KCl-Ringer's (same composition but Na replaced by K). Reagent grade chemicals and glass double distilled water were used.

The voltage-clamp amplifier used was either an Opto-Electronics, Inc. (Tucson, Arizona), model 9733A FET input op-amp or a Functions Module (Irvine, CA) model 380 K. The current was measured as the voltage drop across a 100 kΩ resistor in the feedback loop with a low noise amplifier (Princeton Applied Research model 113). Its output was fed into a real-time spectrum analyzer, (UA 500-1, Nicolet Scientific) monitored on a oscilloscope (Tektronix 502) and recorded on FM tape (Hewlett Packard model 3906). The output of the spectrum analyzer was displayed on an XY oscilloscope and plotted on an XY recorder (MFE model 715). The pseudorandom noise output of the spectrum analyzer was used to drive the positive input of the clamp amplifier to obtain the admittance spectrum.

Results

1. Large Area: 0.071 cm²

Figure 2 shows several spectra of current fluctuations (S_I) on a log-log plot as a function of frequency. The power density decreases with frequency from below 0.5 to about 50 Hz with a $1/f^2$ slope. Above 80 Hz, the power density often increases with frequency, reflecting the effect of membrane capacitance in amplication of amplifier input noise (Poussart, 1971). The upper three curves are averages of 64 spectra measured at three membrane potentials: −35, 0, and 80 mV. The open circuit skin potentials varied from 35 to 47 mV in this skin (summer frog). The total power content fell progressively from the reverse polarized state at −35 mV to the lowest power in the hyperpolarized state at +80 mV. Table 1*A* shows the steady-state currents and slope resistance for the

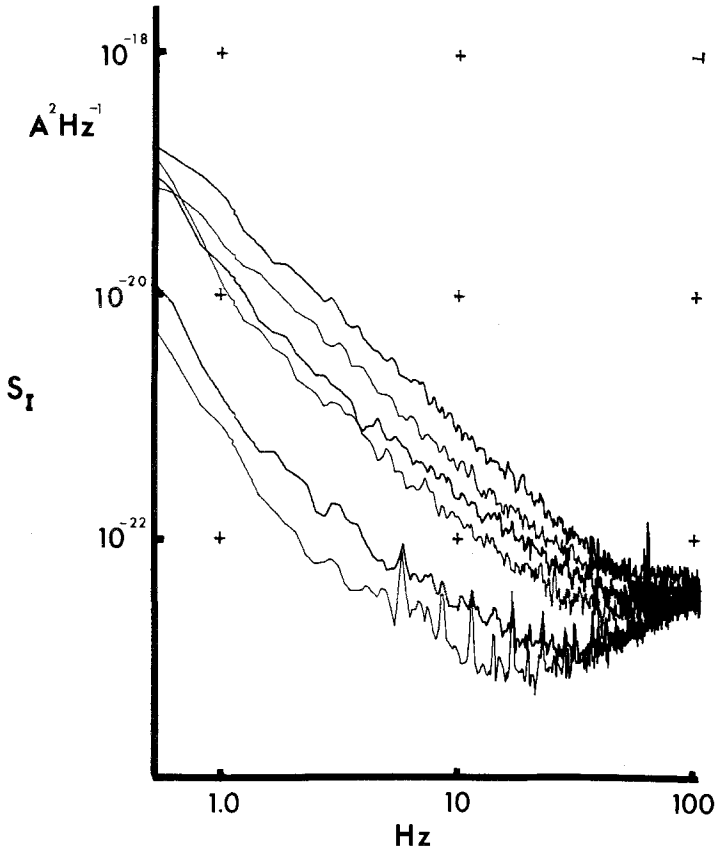

Fig. 2. Power spectra of frog skin current fluctuations from large area (0.071 cm^2) in half-strength sulfate Ringer's. Upper three curves are frog skins in Na-sulfate Ringer's clamped at three potentials (from uppermost): −35 mV (i.e., reverse polarized), 0 mV (short circuit), and +80 mV (hyperpolarized). Each curve is the average of 64 spectra. Lower three curves are from skins in Tris sulfate and clamped at three potentials (from upper to lower): −50 mV (reversed polarized), +50 mV (hyperpolarized), and 0 mV (spontaneous potential)

four clamp levels. These results essentially confirm and extend the findings reported by Segal (1972), by Van Driessche and Borghgraef (1975) and by Lindemann and Van Driessche (1977).

Sodium was replaced in the bathing solution with Tris and the spontaneous potential fell to zero. Current power spectra were again measured at three clamp potentials and the results are shown in the three lower curves in Fig. 2. Currents and slope resistances are given in Table 1*B*. The noise power is strongly dependent on the presence of sodium at the outside border.

Table 1

Clamp Potential (mV)	Steady-state Current ($\mu A\ cm^{-2}$)	Total power from 1 to 10 Hz δI^2 $\times 10^{20}\ A^2\ cm^{-2}$	Chord resistance (kohms cm^2)	Spontaneous PD (mV)	$E(V)$[a] (pmho)
A. Skin in Na-sulfate solutions					
−35	48.1	61	1.57	+41	0.22
0	16.4	31	2.13	+35	0.73
+35	2.0	18	1.52	+38	75
+80	−23.8	15	1.39	+47	0.23
B. Skin bathed in Tris-sulfate solution					
−50	9.05	10.2	5.68	–	
0	0.071	0.60	–	−1.0	
+50	−10.6	1.4	4.74	+3.0	

[a] $E(V)=\sigma_I^2/[I_{Na}(V-V_{Na})(1-\bar{a})]$; *see Discussion.*

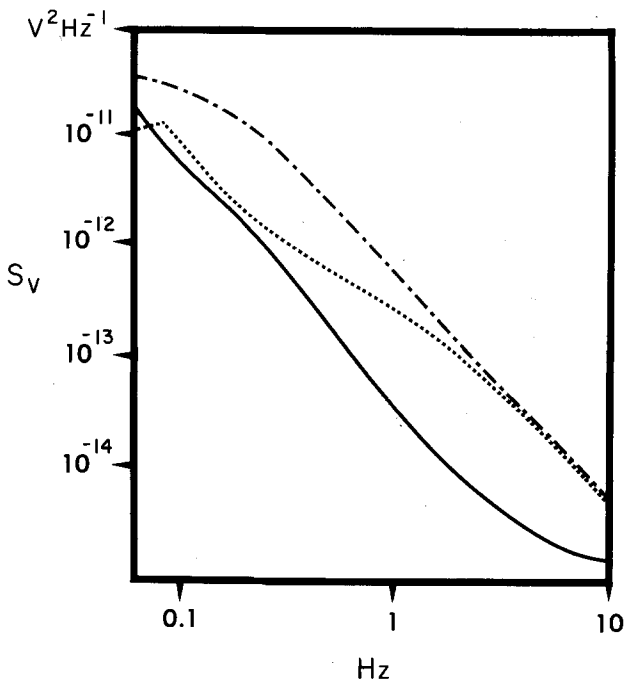

Fig. 3. Voltage power spectra of frog skin (large area)—effect of Na ion and of amiloride in outside bathing solution. Each curve is the average of 16 spectra. Upper curve (— — —) in 55 mM Na sulfate Ringer's, lower curve (solid line) in 60 mM Tris sulfate, and middle curve (· · · · · ·) in 55 mM Na sulfate and 10^{-4} amiloride

Fluctuations in voltage are also dependent upon sodium as shown in Fig. 3. The voltage power spectra (S_V) out to 10 Hz are shown for a skin in three conditions. The upper and lower curves were obtained in the presence and absence of sodium. The curves are very similar in shape to the current power spectra. The middle curve shows the result of amiloride treatment of the same skin bathed in sodium. Treatment with amiloride (concentration 10^{-4} M) resulted in an open circuit potential of zero. Fluctuations were decreased at the low frequencies but not at the higher frequencies, a result also reported by Lindemann and Van Driessche (1977). If the period of exposure to amiloride was not prolonged, the skin potential and current would recover upon washing out the amiloride.

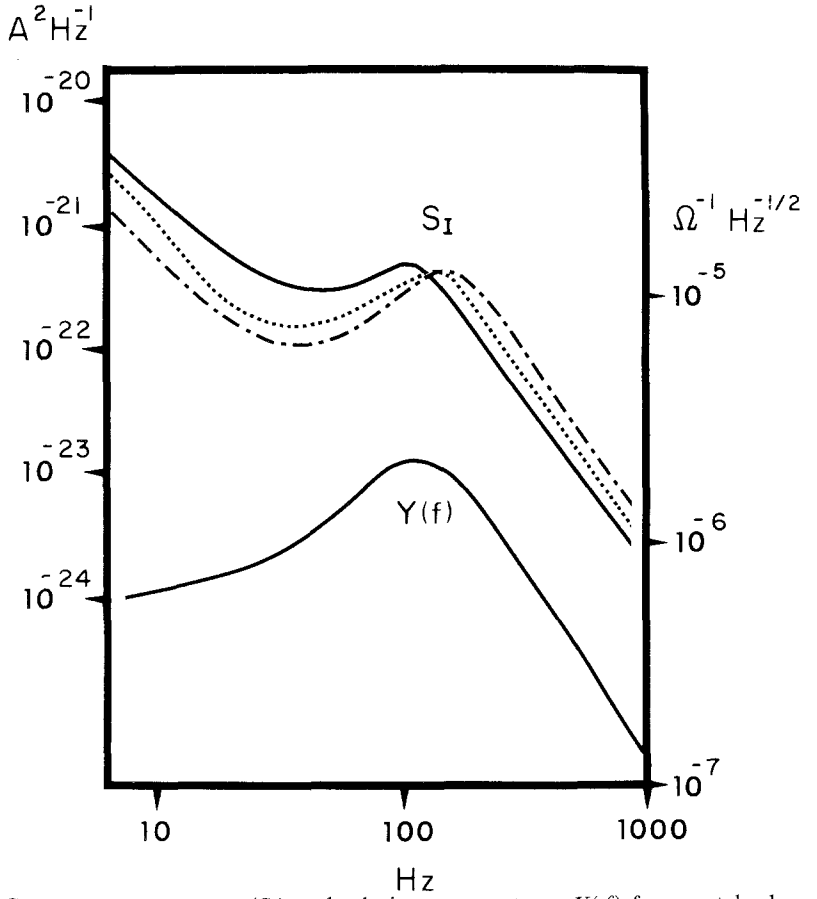

Fig. 4. Current power spectra (S_I) and admittance spectrum $Y(f)$ from patch clamp of frog skin apical surface. Current power spectra during voltage clamp at rest potential of +40 mV (·····), hyperpolarized to +80 mV (———), and reverse polarized to −40 mV (–·–·–). Admittance spectrum, $Y(f)$, was obtained during hyperpolarization to +80 mV. The perfusion solution was NaCl-Ringer's

2. *Small Area: Patch Clamp under Oil, ca. 0.001 cm²*

In the large area preparations, low frequency components completely dominated the fluctuations, and frequencies above 100 Hz were not observed. In contrast, in the patch clamp preparation the most striking observation is the appearance of much higher frequency fluctuations and actually a well defined peak in the current spectrum. In Fig. 4 are shown results for the current power spectra under three clamp levels; hyperpolarized (solid line), at rest potential (dotted) and reverse polarized (dot-dash). The admittance spectrum $|Y(f)|$ shown was virtually identical at the three clamp levels. In this skin, the peak frequency appeared to shift

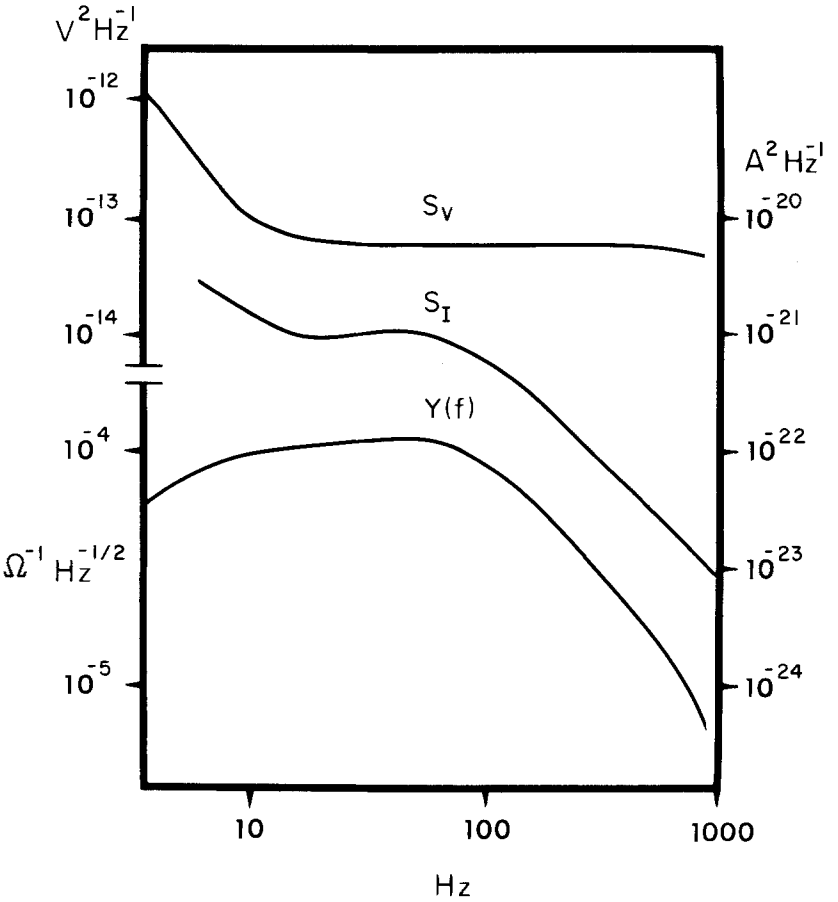

Fig. 5. Patch current (S_I) and voltage (S_v) power spectra and admittance spectrum. Current and power spectra and the admittance spectrum were obtained during clamp at rest potential (+57 mV). Voltage spectrum was obtained during open circuit. Perfusion solution was sulfate Ringer's

slightly with voltage, but in other skins no shift was observed. The voltage power spectrum was flat above 50–80 Hz.

In some skins, even ones with relatively high potentials, the peaks were not apparent in either the current or admittance spectra, as shown in Fig. 5. The voltage spectrum is flat and the relation:

$$S_I = |Y(f)|^2 S_V \tag{1}$$

appears to hold (*cf.* Poussart, 1971). Although the current spectrum shows a final limiting slope of $1/f^2$, the break is too sharp to be strictly Lorenztian. It would appear that this curve is higher than first order, and behaves as would a damped oscillator. The appearance of the peak was

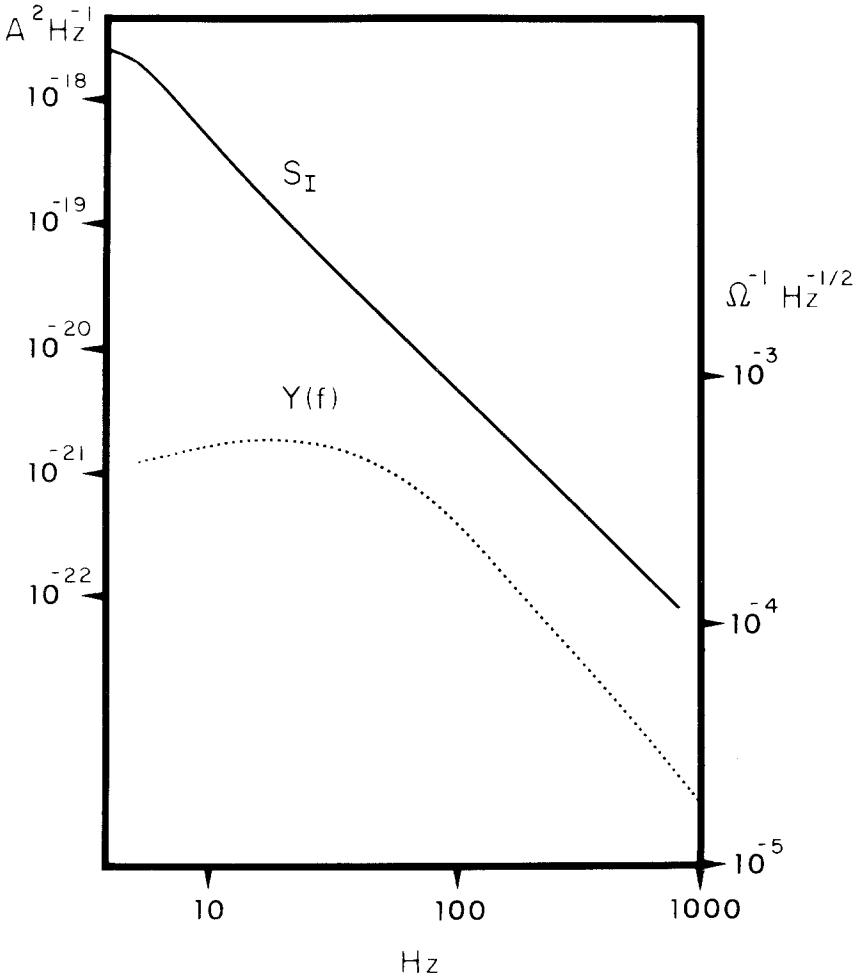

Fig. 6. Patch clamp current power and admittance spectra during voltage clamp at spontaneous potential in KCl (0.0 mV). The perfusion solution was KCl solution

similar in either chloride or sulfate Ringer's. In this particular experiment, sulfate was the major anion, but similar flattening of the peak was also observed in chloride Ringer's. In skins with poor potentials peaks were rarely seen.

The resonance peak disappears with the substitution of K^+ ion for Na^+ ion in the patch pipette. This is shown in Fig. 6. The peak in both the current power spectrum and admittance spectrum has disappeared. The fact that the high frequency peak has disappeared with the removal of the sodium ion indicates that the peak may be attributable to the sodium channels and is not associated with a gross mechanical resonance in the system.

Discussion

Several considerations indicate that the patch clamp results are due to the epithelium and are not artifacts. Extensive control experiments using the same feedback system to clamp dummy equivalent circuits of resistors and capacitors never gave rise to resonance peaks (except for the amplification of input voltage noise at much higher frequencies). In addition, the resonance peaks shifted in frequency with the clamp potential and depended on the presence of sodium. Skins, some with poor potentials, exhibited only small peaks or none at all. These observations argue for attributing the peaks to the epithelial membrane. Different clamp amplifiers and clamp arrangements gave essentially identical results. Therefore, the results appear to be properties of the epithelium *per se*.

The double pipette patch clamp was used instead of a single pipette system in order to avoid a large series resistance between the control point and the membrane. This raises the question: Is the potential sensed under the potential pipette the same as the potential under the current pipette? This problem has been studied in two ways with J.E. Clarke (*unpublished*). First of all, a single large (100 μm) pipette was used to inject current, and a microelectrode was positioned with its tip on the surface under the orifice of the current pipette. This arrangement also exhibited peaks in the current power spectrum. Secondly, the spread of current under the oil was observed. Upon injection of current pulses, the response in potential at the surface fell off exponentially with distance. The "space constant" was about 770 μm. Although this preparation is a two dimensional system, since the current source is relatively large the

potential spread is considerable, and it appears that the side-by-side pipette arrangement should lead to less than a 10% attenuation of the potential under the potential electrode.

The appearance of high frequency fluctuations in the patch clamp preparation and its absence in records from "large" areas requires discussion. The difference probably arises from the fact that the space clamp of large pieces of frog skin bathed in Ringer's is not ideal. Thus, any given unit noise current source has in parallel with it not only its own intrinsic capacitance but also the capacitance of the area of the effective space constant under the clamp. Thus, the time constant of the fluctuations in the large area preparation reflects the time constants of the distributed network under the spatially averaged clamp region. The patch clamp reflects more closely the kinetics of the individual unit noise sources. In effect, the large area clamp represents a spatial average which tends to filter out the high frequency components.

Nevertheless, the low frequency effects probably reflect membrane phenomena, although instrumental factors and extraneous noise contributions appear to be more severe at low frequencies than at high (Strandberg & Hammer, 1975). Lindemann (1976) analyzed results at low frequencies, assuming that this component has a Lorentzian character, although distinct Lorentzian corner frequencies could be estimated only roughly. Lindemann and Van Driessche (1977) analyzed results in the presence of amiloride at low frequencies in which distinct corners could be observed.

A method has been devised by Begenisich and Stevens (1975) and elaborated by Chen (1976) to identify single state *vs.* multistate channel conductance mechanisms in nerve by noise analysis. An experimentally measureable function to estimate the single channel K conductance is given by Chen (1976):

$$E(V)=\frac{\sigma_I^2}{I_K(1-\bar{a})(V-V_K)}. \tag{2}$$

This function, for a multistate model is proportional to the single channel conductance $\bar{g}_K$:

$$\bar{g}_K\,\gamma(V)=E(V) \tag{3}$$

where

$$\gamma(V)=\frac{[\overline{a^2}-(\bar{a})^2]}{[\bar{a}-(\bar{a})^2]} \tag{4}$$

and

$$\overline{a^2} = \Sigma\, a_j^2\, p_j^s, \quad j = 0, x \tag{5}$$

$$\bar{a} = \Sigma\, a_j p_j^s, \quad j = 0, x. \tag{6}$$

Also p_j^s is the steady-state probability that a system is in state j and $a_j \bar{g}_K$ is the unit conductance in state j ($a_j > 1$). Chen has pointed out that in a single-state model, $\gamma(V)$ is unity and $E(V) \equiv \bar{g}_K$. However, for a multistate channel, $\gamma(V)$ would be a function of the potential. Thus, dependence of $E(V)$ on potential would indicate a multistate mechanism.

If, as has been suggested, sodium transport is mediated through pores, this test could be applied to the data in Table 1. For this test, let us assume that $\bar{a}$ is estimated by the ratio g_{Na}/g_{Na}^m where g_{Na}^m is the maximal conductance, for example in the presence of novobiocin (Johnston & Hoshiko, 1971) or other stimulating agents (Lindemann, 1976). This ratio may range from 1 : 2 to 1 : 5. Lindemann (1976) has shown that g_{Na} is dependent upon the sodium concentration and hence fluctuations in the conductance may reflect local fluctuations in sodium concentration. The variance σ_I^2 is obtained by integration of the power spectrum attributable to the sodium channel. It should be the integral of the difference between the power spectrum in the presence and in the absence of sodium. Over the frequency band of interest (>1 Hz) the additional noise contribution of nonsodium noise is lower by more than an order of magnitude and the difference spectrum was not necessary. The quantity $(V - V_{Na})$ is the displacement from the equilibrium potential and is less easily defined. If we identify I_{Na} as a linear function of $(V - V_{Na})$ with zero intercept, then the open circuit potential can be taken to represent V_{Na} and some proportion of any displacement from that value would appear across the apical membrane. Thus, $(V - V_{Na})$ taken as the displacement from open circuit potential would overestimate the actual $(V - V_{Na})$ at the apical border. This would tend to underestimate $E(V)$, but should be within an order of magnitude. With these cautions, it is instructive to examine $E(V)$ for $\bar{a} = 1/5$ as shown in Table 1. The values range from 0.2 to 75.0 pmho. In nerve, Begenisich and Stevens (1975) report a single channel conductance of 4 pmho. Lindemann and Van Driessche (1977) estimate single channel currents of 0.3 to 0.5 pA, which for a 0.1 V driving force would mean conductances of 3–5 pmho. However, the proper value to be used for the driving voltage is problematic, and the conductances would be larger for smaller voltages. The main point from the data in Table 1 is that $E(V)$ is indeed potential dependent. Despite possible errors due to selection of an incorrect value

of $(V-V_{Na})$, the magnitude of the range of values of $E(V)$ is too large to be accounted for in this way. Thus, low frequency behavior appears to indicate a multistate channel process.

The appearance of high frequency fluctuations is the distinctive feature of the small area or patch clamp. The form of the high frequency phenomena depends upon the presence of sodium. Absence of sodium leads to the disappearance of the peak in the admittance spectrum. Even in skins with no pronounced peak, the corner in the current power spectrum was too sharp to be Lorentzian. These higher frequency phenomena including peaks may be interpreted at two levels: first, in terms of an equivalent electrical circuit and, second, in terms of a molecular-kinetic model. The first level is relatively straight-forward, but the second would require specific assumptions about molecular or kinetic mechanisms. Such a molecular interpretation has been attempted by Lindemann and Van Driessche (1977). Electrical analysis is important in order to assess how apical membrane fluctuations may or may not have been modified by the electrical properties of the surrounding structures and the input characteristics of the detection system. If a simple series *RLC* circuit is assumed, then from the resonance frequency, half power points and the admittance at resonance, R, L and C can be calculated. In the case of the admittance curve in Fig. 4, resonance is at 118 Hz, and $R_0=4.545\times10^2\,\Omega\,\mathrm{cm}^2$, $L=0.761\,\mathrm{H\,cm}^2$, $C=2.4\times10^{-6}\,\mathrm{F\,cm}^2$. The presence of a passive parallel conductive pathway should not alter the resonant frequency. The value of the capacitance is close to the value reported by Smith (1975) for frog skin ($2.39\,\mu\mathrm{F\,cm}^{-2}$). Smith also reports small inductive effects at low frequencies but gave no values for inductance.

Appearance of inductive effects is not unexpected in retrospect in view of the electrical excitability of the apical border (Finkelstein, 1961; 1964; Lindemann & Thorns, 1967; Candia, 1970). Such a time-varying resistance can be modeled as an equivalent inductance as discussed by Mauro (1961) and Mauro *et al.*, (1970). Excitability is reported (Finkelstein, 1964) to vary from skin to skin and may correspond to the variable appearance of resonance peaks in the power spectrum.

I would like to thank Dr. L.E. Moore and W.L. Schultz for advice and helpful criticism. This work was supported by a grant from the U.S. Public Health Service (AM-05865).

References

Begenisich, T., Stevens, C.F. 1975. How many conductance states do potassium channels have? *Biophys. J.* **15**:843

Candia, O.A. 1970. The hyperpolarizing region of the current-voltage curve in frog skin. *Biophys. J.* **10**:323

Chen, Y. 1976. Differentiation of channel models by noise analysis. *Biophys. J.* **16**:965

Conti, F., DeFelice, L.J., Wanke, E. 1975. Potassium and sodium ion current noise in the membrane of the squid axon. *J. Physiol. (London)* **248**:45

Derksen, H.E. 1965. Axon membrane voltage fluctuations. *Acta Physiol. Pharmacol. Neerl.* **13**:373

Derksen, H.E., Verveen, A.A. 1966. Fluctuations of resting neural membrane potential. *Science* **151**:1388

Finkelstein, A. 1961. Electrical excitability of isolated frog skin. *Nature (London)* **190**:1119

Finkelstein, A. 1964. Electrical excitability of isolated frog skin and toad bladder. *J. Gen. Physiol.* **47**:545

Fishman, H.M. 1975. Rapid complex impedance measurements of squid axon membrane via input-output cross correlation function. *In:* Proceedings of First Symposium on Testing and Identification of Nonlinear Systems. G.D. McCann and P.Z. Marmarelis, editors. p. 257. California Institute of Technology, Pasadena

Fishman, H.M., Moore, L.E., Poussart, D.J.M. 1975. Potassium-ion conduction noise in squid axon membrane. *J. Membrane Biol.* **24**:305

Fishman, H.M., Poussart, D.J.M., Moore, L.E. 1975. Noise measurements in squid axon membrane. *J. Membrane Biol.* **24**:281

Hoshiko, T. 1975. Power density spectra (PDS) of frog skin. *J. Gen. Physiol.* **66**:16*a*

Hoshiko, T., Moore, L.E. 1978. Fluctuation analysis of epithelial membrane kinetics. *In:* Membrane Transport Kinetics. Vol. 1, p. 179. J.F. Hoffman, editor. Raven Press, New York

Johnston, K., Hoshiko, T. 1971. Novobiocin stimulation of frog skin current and some metabolic consequences. *Am. J. Physiol.* **220**:702

Koefoed-Johnson, V., Ussing, H.H. 1958. The nature of the frog skin potential. *Acta Physiol. Scand.* **42**:298

Lindemann, B. 1978. The mechanism of Na-uptake through Na-selective channels in the epithelium of frog skin. *In:* Membrane Transport Processes. Vol. 1, p. 155. J.F. Hoffman, editor. Raven Press, New York

Lindemann, B., Thorns, U. 1967. Fast potential spike of frog skin generated at the outer surface of the epithelium. *Science* **158**:1473

Lindemann, B., VanDriessche, W. 1977. Sodium-specific membrane channels of frog skin are pores: Current fluctuations reveal high turnover. *Science* **195**:292

Mauro, A. 1961. Anomalous impedance, a phenomenological property of time-variant resistance. *Biophys. J.* **1**:353

Mauro, A., Conti, F., Dodge, F., Schor, R. 1970. Subthreshold behavior and phenomenological impedance of the squid giant axon. *J. Gen. Physiol.* **55**:497

Menninger, J.R., Snell, F.M., Spangler, R.A. 1960. Voltage clamp for biological investigations. *Rev. Sci. Instr.* **31**:519

Poussart, D.J.M. 1969. Nerve membrane current noise: Direct measurements under voltage clamp. *Proc. Nat. Acad. Sci. USA* **64**:95

Poussart, D.J.M. 1971. Membrane current noise in lobster axon under voltage clamp. *Biophys. J.* **11**:211

Segal, J.R. 1972. Electrical fluctuations associated with active transport. *Biophys. J.* **12**:1371

Seldin, J.P., Hoshiko, T. 1966. Ionic requirement for epinephrine stimulation of frog skin gland secretion. *J. Exp. Zool.* **163**:111

Smith, P.G. 1975. Frequency dependence of the frog skin impedance. *Biochim. Biophys. Acta* **375**:124

Strandberg, M.W.P., Hammer, E.I. 1975. Current fluctuation noise in toad urinary bladder during active transport of sodium ions. *J. Appl. Phys.* **46**:3661

Ussing, H.H., Koefoed-Johnson, V. 1956. Nature of the frog skin potential. *Abstr. Comm. XX Internat. Physiol. Congr., Brussels*, p. 611

Van Driessche, W., Borghgraef, R. 1975. Noise generated during ion transport across frog skin. *Arch. Int. Physiol. Biochim.* **83**:140

Wanke, E., DeFelice, L.F., Conti, E. 1974. Voltage noise, current noise and impedance in space clamped squid giant axon. *Pfluegers Arch.* **347**:63